ARTICLE

De Novo Missense Mutations in *DHX30* Impair Global Translation and Cause a Neurodevelopmental Disorder

Davor Lessel,[1,2,28,29,*] Claudia Schob,[1,28,29] Sébastien Küry,[3] Margot R.F. Reinders,[4] Tamar Harel,[5] Mohammad K. Eldomery,[6] Zeynep Coban-Akdemir,[6] Jonas Denecke,[7] Shimon Edvardson,[8,9] Estelle Colin,[10,11] Alexander P.A. Stegmann,[4,12] Erica H. Gerkes,[13] Marine Tessarech,[10,11] Dominique Bonneau,[10,11] Magalie Barth,[10,11] Thomas Besnard,[3] Benjamin Cogné,[3] Anya Revah-Politi,[14] Tim M. Strom,[15,16] Jill A. Rosenfeld,[6] Yaping Yang,[6] Jennifer E. Posey,[6] LaDonna Immken,[17] Nelly Oundjian,[18] Katherine L. Helbig,[19] Naomi Meeks,[20,21] Kelsey Zegar,[20,21] Jenny Morton,[22] the DDD study, Jolanda H. Schieving,[23] Ana Claasen,[24] Matthew Huentelman,[24] Vinodh Narayanan,[24] Keri Ramsey,[24] C4RCD Research Group, Han G. Brunner,[4] Orly Elpeleg,[5,9] Sandra Mercier,[3] Stéphane Bézieau,[3] Christian Kubisch,[1,2] Tjitske Kleefstra,[4] Stefan Kindler,[1] James R. Lupski,[6,25,26,27] and Hans-Jürgen Kreienkamp[1,*]

DHX30 is a member of the family of DExH-box helicases, which use ATP hydrolysis to unwind RNA secondary structures. Here we identified six different *de novo* missense mutations in *DHX30* in twelve unrelated individuals affected by global developmental delay (GDD), intellectual disability (ID), severe speech impairment and gait abnormalities. While four mutations are recurrent, two are unique with one affecting the codon of one recurrent mutation. All amino acid changes are located within highly conserved helicase motifs and were found to either impair ATPase activity or RNA recognition in different *in vitro* assays. Moreover, protein variants exhibit an increased propensity to trigger stress granule (SG) formation resulting in global translation inhibition. Thus, our findings highlight the prominent role of translation control in development and function of the central nervous system and also provide molecular insight into how DHX30 dysfunction might cause a neurodevelopmental disorder.

Introduction

ATP-dependent unwinding of RNA secondary structures by RNA helicases (RHs) is required for most aspects of RNA metabolism, including synthesis, nuclear processing and export, translation, and storage and decay of RNA, as well as ribonucleoprotein (RNP) assembly.[1–3] Six superfamilies of RHs are known,[2] with superfamily 2 containing more than 50 human members characterized by a DExD or DExH signature in their Walker B motif, thus termed DDX and DHX proteins, respectively.[4] Several RHs have been assigned to multiple cellular functions, often operating in large RNP complexes, while others appear to be restricted to a particular cellular process.[2] Whereas a large body of structural and functional data has been accumulated for RHs from model organisms, such as the yeast DExH protein Prp43, for most human RHs the exact function remains unknown.

Human genetic studies have recently begun to address the pathological relevance of altered RH function; thus, somatic mutations in *DDX3X* (MIM: 300160) observed in various tumors were found to disrupt global translation.[5]

[1]Institute of Human Genetics, University Medical Center Hamburg-Eppendorf, 20246 Hamburg, Germany; [2]Undiagnosed Disease Program at the University Medical Center Hamburg-Eppendorf (UDP-UKE), Martinistraße 52, 20246 Hamburg, Germany; [3]CHU Nantes, Service de Génétique Médicale, 9 quai Moncousu, 44093 Nantes Cedex, France; [4]Department of Human Genetics, Radboud University Medical Center, 6500 HB Nijmegen, the Netherlands; [5]Department of Genetic and Metabolic Diseases, Hadassah-Hebrew University Medical Center, Jerusalem, Israel 9112001; [6]Department of Molecular and Human Genetics, Baylor College of Medicine, Houston, TX 77030, USA; [7]Department of Pediatrics, University Medical Center Eppendorf, 20246 Hamburg, Germany; [8]Pediatric Neurology Unit, Hadassah-Hebrew University Medical Center, Jerusalem, Israel 9112001; [9]Monique and Jacques Roboh Department of Genetic Research, Hadassah-Hebrew University Medical Center, Jerusalem, Israel 9112001; [10]Department of Biochemistry and Genetics, University Hospital, 49933 Angers Cedex 9, France; [11]Equipe MitoLab, CNRS UMR 6015, Inserm U1083, Institut MitoVasc of Angers, CHU Bât IRIS/IBS, Rue des Capucins, 49933 Angers Cedex, France; [12]Department of Clinical Genetics, Maastricht University Medical Centre, Maastricht, the Netherlands; [13]Department of Genetics, University of Groningen, University Medical Center Groningen, Groningen, the Netherlands; [14]Institute for Genomic Medicine, Columbia University, New York, NY 10032, USA; [15]Institute of Human Genetics, Helmholtz Zentrum München, 85764 Neuherberg, Germany; [16]Institute of Human Genetics, Technical University of Munich, 81675 Munich, Germany; [17]Clinical Genetics, Specially for Children, Austin, TX 78723, USA; [18]Valley Hospital, Ridgewood, NJ, USA; [19]Division of Clinical Genomics, Ambry Genetics, Aliso Viejo, California, USA; [20]Division of Clinical Genetics and Metabolism, Department of Pediatrics, University of Colorado School of Medicine, Aurora, CO, USA; [21]Clinical Genetics, Children's Hospital Colorado, Aurora, CO, USA; [22]West Midlands Regional Clinical Genetics Service and Birmingham Health Partners, Birmingham Women's and Children's NHS Foundation Trust, B15 2TG Birmingham, UK; [23]Department of Pediatric Neurology, Donders Institute for Brain, Cognition and Behaviour, Radboud University Medical Center, Nijmegen, the Netherlands; [24]Center for Rare Childhood Disorders, Translational Genomics Research Institute, Phoenix, Arizona, USA; [25]Texas Children's Hospital, Houston, TX 77030, USA; [26]Baylor Genetics Laboratories, Baylor College of Medicine, Houston, TX 77030, USA; [27]Human Genome Sequencing Center, Baylor College of Medicine, Houston, TX 77030, USA

[28]First author
[29]These authors contributed equally to this work
*Correspondence: d.lessel@uke.de (D.L.), kreienkamp@uke.de (H.-J.K.)
https://doi.org/10.1016/j.ajhg.2017.09.014

Moreover, germline mutations in the same gene are associated with intellectual disability (MIM: 300958),[6] pointing to a role of translational control in proper development and function of the nervous system.

Here we describe disease-causing *de novo* missense mutations in *DHX30* (MIM: 616423, RefSeq NM_138615.2) in individuals affected by intellectual disability and global developmental delay. DHX30 belongs to the DExH family of RNA helicases, and has until now mostly escaped scientific attention. We show that DHX30 is indeed an RNA-dependent ATPase, and that all mutations interfere with either RNA binding or ATPase activity. Importantly, protein variants of DHX30 interfere also with global translation by inducing the formation of stress granules.

Material and Methods

Research Subjects
Written informed consent for all subjects was obtained in accordance with protocols approved by the respective ethics committees of the institutions involved in this study.

Genetic Analysis
Some of the investigators presenting affected individuals in this study were connected through GeneMatcher, a web-based tool for researchers and clinicians working on identical genes.[7] Trio whole-exome sequencing (trio-WES) experiments, data annotation, and interpretation were performed in nine different centers with slightly different procedures using methods that were described previously. Briefly, trio-WES in families A, C, D, E, J, and L were performed with a SureSelect Human All Exon (Agilent, Santa Clara, CA, USA), and sequenced on a HiSeq2000, HiSeq2500 or HiSeq4000 platform (Illumina, San Diego, CA, USA), as described before.[8–13] Trio-WES in families B, H, and K was performed with a SOLiD-Optimized SureSelect Human Exome Kit (Agilent version 2, 50 Mb), followed by SOLiD 4 System sequencing (Life Technologies) as previously described.[14,15] Trio-WES in family I was performed using the SeqCapEZ VCR 2.0 (Roche NimbleGen) and sequenced on the HiSeq 2000 Sequencer (Illumina, San Diego, CA, USA) as previously described.[16] Genetic analyses in families F and G were described before.[17] All putative *de novo* variants were validated and confirmed by Sanger sequencing, by standard procedure.

Expression Constructs
cDNA coding for transcript variant 1 of human DHX30 was obtained from Origene; the DHX30 coding sequence was subcloned into EcoRI/SmaI sites of pEGFP-C3 (Clontech), allowing for expression of DHX30-WT carrying an N-terminal GFP-tag (GFP-DHX30). In parallel, several constructs were generated in pEGFP-N2, leading to expression of DHX30 variants carrying a C-terminal GFP-tag (DHX30-GFP); in particular, we generated a construct corresponding to transcript variant 3; the protein product of this cDNA carries a putative N-terminal mitochondrial targeting sequence. Missense mutations found in affected individuals were introduced into the pEGFP-C3 based vector, and into the mitochondrial construct using Quick-Change II site directed mutagenesis kit (Agilent, Waldbronn, Germany), with mutagenic oligonucleotides designed based on the Quick-Change

instruction manual. All constructs were verified by Sanger sequencing.

Cell Culture, Transfection, and Immunocytochemistry
Human embryonic kidney 293T (HEK293T) and human bone osteosarcoma epithelial (U2OS) cells were grown on cell culture dishes and coverslips, respectively, utilizing Dulbecco's Modified Eagle Medium (DMEM) supplemented with 10% fetal bovine serum (FBS). Cells were transfected with TurboFect transfection reagent (ThermoFisher Scientific) according to the manufacturer's recommendations. Fixation of U2OS cells and immuno-cytochemical analysis was performed as previously described[18] employing the following antibodies at manufacturers' recommended dilutions: anti-DHX30 rabbit polyclonal (Bethyl, #A302-218A), anti-DDX3X mouse monoclonal (BioLegend, #658602), anti-Mitochondria mouse monoclonal (Abcam, #ab3298), anti-puromycin mouse monoclonal (Millipore, #MABE343), and goat anti-mouse, anti-rat, and anti-rabbit IgG coupled to either Alexa Fluor 488, Alexa Fluor 546, or Alexa Fluor 635, respectively (ThermoFisher Scientific). A custom made anti-ATXN2 rat monoclonal antibody was used at a 1:10 dilution. Recombinant DHX30 fusion proteins were directly visualized via their GFP-tag. Coverslips were mounted with ProLong Diamond Antifade Mountant with DAPI (ThermoFisher Scientific). Images were acquired utilizing a confocal microscope (Leica TCS SP8, 63x/1.25 objective) and processed using ImageJ, Corel Paint Shop Pro X, macromedia FreeHand MX and PowerPoint software.

ATPase Assay
Transfected HEK293T cells were lysed in 1 mL of radioimmunoprecipitation assay (RIPA) buffer (50 mM Tris-HCl pH 8.0; 150 mM NaCl; 0.1% SDS; 0.5% sodium deoxycholate; 1% NP-40; 5 mM EDTA) and lysates were cleared by centrifugation at 20,000 x g for 20 min at 4°C. GFP-containing proteins were purified from the supernatant by immunoprecipitation using 20 μl of GFP-Trap_A matrix (Chromotek, Munich, Germany). Precipitates were washed twice in RIPA buffer, and twice in phosphate free ATPase assay buffer (40 mM KCl; 35 mM HEPES pH 7.5; 5 mM MgCl$_2$; prepared in plastic ware to avoid phosphate contamination). Precipitates were then incubated in 50 μl phosphate free buffer supplemented with 2 mM ATP and 2 mM DTT at 30°C for 30 min (for assaying ATPase activity in the absence of exogenous RNA). After brief centrifugation (1 min, 1000 x g), the supernatant was removed and precipitate samples were incubated in phosphate free buffer containing 2 mM ATP; 2 mM DTT, and 100 μg/ml yeast RNA for 30 min at 30°C (for assaying ATPase activity in the presence of exogenous RNA). The amount of free phosphate released by ATP hydrolysis was determined photometrically using Biomol Green reagent (Enzo Life Sciences, Lörrach, Germany). Subsequently, the amount of bead-attached DHX30 protein was determined by western blotting using anti-GFP (Covance). In each case, ATPase activity was normalized to the amount of GFP-tagged DHX30 protein attached to the GFP-trap matrix.

RNA Immunoprecipitation
Immunoprecipitation of recombinant proteins from lysates of transfected HEK293T cells via GFP-Trap_A (Chromotek), RNA purification from precipitates and real-time PCR with TaqMan probes were essentially performed as previously described.[18] TaqMan Gene Expression Assays (ThermoFisher Scientific) for the

Table 1. Clinical Characteristics of Affected Individuals with *DHX30* Alterations

Clinical findings	Proband A	Proband B	Proband C	Proband D	Proband E	Proband F	Proband G	Proband H	Proband I	Proband J	Proband K	Proband L
Sex	Female	Male	Female	Female	Male	Female	Female	Female	Female	Male	Female	Male
Age at last examination (years)	3 9/12	13	6 3/12	8	17	14	14 2/12	8	6 1/12	4 8/12	6 5/12	4 8/12
Intellectual disability	+	+	+	+	+	+	+	+	+	+	+	+
Age of first words (years)	1 8/12	4	–	–	–	–	–	–	–	–	–	–
Speech ability	20 words	4 words	non-verbal	non-verbal	non-verbal	non-verbal	non-verbal	non-verbal	non-verbal	non-verbal	non-verbal	non-verbal
Motor development delay	+	+	+	+	+	+	+	+	+	+	+	+
Muscular hypotonia	+	+	+	+	+	+	+	+	+	+	+	+
Age of walking (years)	2 8/12	6	–	–	6	–	3	–	–	–	5	8
Gait abnormalities	ataxic	ataxic	no independent walking	no independent walking	ataxic; only short distances independent	no independent walking	ataxic	no independent walking	no independent walking	no independent walking	ataxic	ataxic
Autistic features	+	–	+	–	+	+	+	–	+	–	+	–
Sleep disturbance	+	+	+	+	–	–	+	+	+	–	–	–
Seizures	+	–	–	+	–	–	–	–	+	–	–	–
Feeding difficulties	+	+	–	–	+	+	+	+	+	+	–	+
Strabismus	+	–	+	–	–	–	–	–	+	+	+	+
Joint hypermobility	+	–	+	–	+	+	–	–	+	–	+	–
Cerebral MRI anomalies	–	–	–	delayed myelination, cerebellar atrophy, enlarged ventricles	cortical atrophy, dilated ventricles	mild cerebral atrophy	delayed myelination	cerebral atrophy, delayed myelination, dilated ventricles	cerebral atrophy	delayed myelination, dilated ventricles, corpus callosal abnormalities	delayed myelination, cerebellar atrophy, dilated ventricles	delayed myelination, cerebellar atrophy, dilated ventricles
***DHX30* alteration**	c.1478G>A p.Arg493His	c.1478G>A p.Arg493His	c.1685A>G p.His562Arg	c.2342G>A p.Gly781Asp	c.2342G>A p.Gly781Asp	c.2344C>T p.Arg782Trp	c.2344C>T p.Arg782Trp	c.2344C>T p.Arg782Trp	c.2353C>T p.Arg785Cys	c.2353C>T p.Arg785Cys	c.2353C>T p.Arg785Cys	c.2354G>A p.Arg785His

+, present; –, absent;
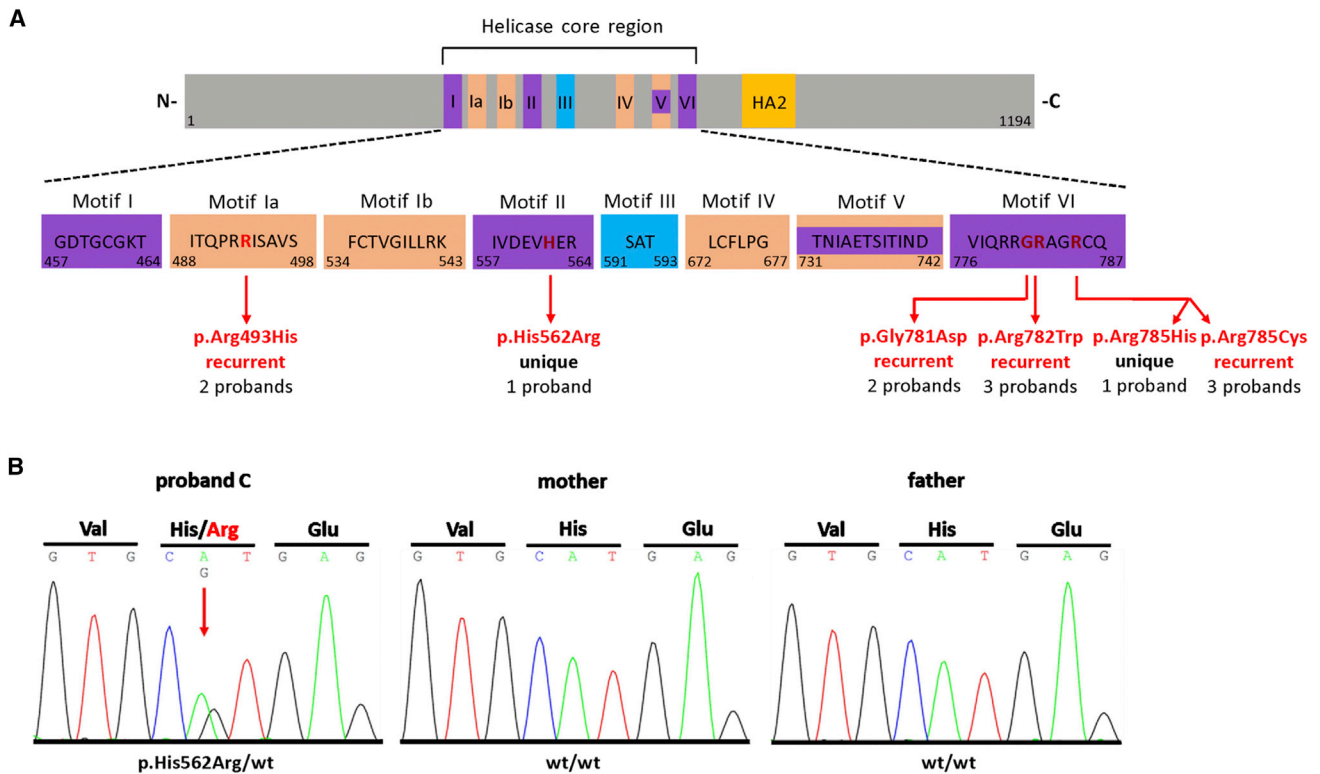
Figure 1. Identified Variants Are Localized within Conserved Helicase Motifs of DHX30

(A) Top: Schematic protein structure of DHX30 showing conserved motifs of the helicase core region and the helicase associated domain (HA2). Nucleotide-interacting motifs (I, II, and VI) are shown in purple, nucleic acid-binding motifs (Ia, Ib, and IV) in orange, motif V, which binds nucleic acid and interacts with nucleotides, in purple and orange, and motif III, which couples ATP hydrolysis to RNA unwinding, in blue. (N- N terminus; C- C terminus). Bottom: Amino acids within conserved motifs of the helicase core region. The position of the first and last amino acid within each motif is denoted below left and right, respectively. The position of the *de novo* mutations identified in this study are marked with vertical red arrows and shown in red.

(B) Sanger sequence electropherograms of parts of *DHX30* after PCR amplification of genomic DNA of the affected individual C and his parents, exemplifying *de novo* status of the mutations identified here. The amino acid translation is shown in the three-letter code above the DNA sequence. The red arrow indicates the heterozygous mutation at c.1685A>G, (p.His562Arg), present only in the DNA sample of the affected individual.

following human genes were used: *AES* (Assay ID Hs01081012_m1), *B4GAT1* (Hs04194311_s1) and *MRPL11* (Hs00601653_g1).

Puromycin Incorporation Assay

Transfected U2OS cells were pulse labeled with puromycin (Invitrogen; 1 μg/ml) for 30 min. Immuno-cytochemistry was performed as described above.

Statistics

Statistical evaluation was performed depending on the experiment by either two-tailed unpaired Student's t test or ANOVA followed by Dunnett's multiple comparisons test using Prism 6 (GraphPad), as specifically indicated for each experiment in figure legends. P values expressed as *($p < 0.05$), **($p < 0.01$), and ***($p < 0.001$) were considered significant. ns, indicates no significant difference between the groups.

Results

Using trio whole-exome sequencing (WES) or in a single case using singleton-WES followed by targeted Sanger-resequencing, we identified six different *de novo* mutations in *DHX30* in 12 unrelated individuals affected by GDD and ID. Individuals A and B

spoke 20 and 4 words, respectively, whereas the others remained non-verbal. All individuals had delayed milestones of motor development. Six have never learned to walk without support, whereas the others have an ataxic gait and are only able to walk short distances. Further, subtle and only partially overlapping facial dysmorphisms were observed. The clinical phenotype further included muscular hypotonia in all affected individuals, feeding difficulties and brain anomalies on MRI in nine, autistic features and sleep disturbances in seven, and strabismus and joint hypermobility in six individuals (Figure S1, Table 1 and Supplemental Note).

DHX30 belongs to the DExH family of RHs. Within its helicase core region, there are eight highly conserved motifs which are, based on homology to other superfamily 2 helicases,[19] predicted to mediate either ATP binding/hydrolysis or RNA recognition (Figure 1 and Figure S2). Interestingly, each mutation reported herein leads to a substitution of a conserved residue within one of these motifs. We predicted the functional relevance of these residues based on homology to other superfamily 2 helicases[19] and on published structures of the RH Prp43.[20] In more detail, c.1478G>A, (p.Arg493His) identified in two individuals affects motif Ia, and Arg493 is likely a key residue mediating RNA binding.[1] All other amino acid substitutions identified lie within motifs
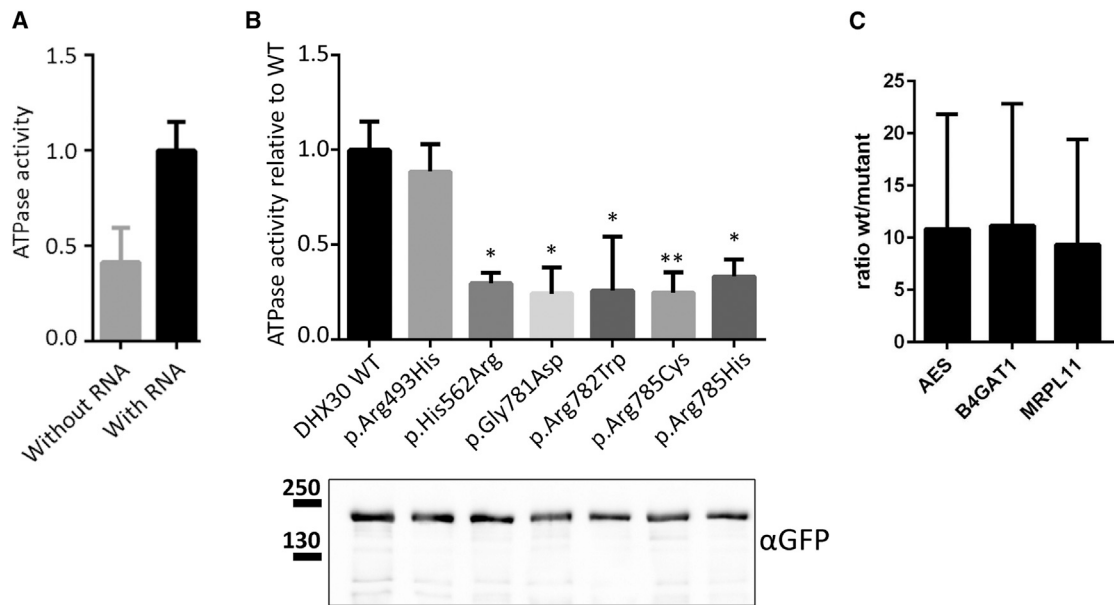
Figure 2. Recombinant Protein Variants of DHX30 Affect Either ATPase Activity or RNA-Binding

(A) GFP-tagged DHX30-WT was immunoprecipitated from HEK293T cell lysates using GFP-Trap_A matrix and assayed for ATPase activity first in the absence and then in the presence of exogenous RNA. Values are normalized on ATPase activity obtained with RNA.

(B) ATPase assays were repeated for WT and protein variants of GFP-DHX30 in the presence of RNA. In each case, ATPase activity was normalized to the amount of DHX30 protein, as determined by western blotting using anti-GFP. *,**: significantly different from DHX30-WT (*$p < 0.05$; **$p < 0.01$; n = 4; ANOVA, followed by Dunnett's multiple comparisons test).

(C) RNAs extracted from GFP-Trap_A precipitates of DHX30-WT, p.Arg493His, and GFP-mCherry fusion proteins obtained from transfected HEK293T cells were subjected to gene-expression analysis using TaqMan probes for specific human mRNAs. The bar graph displays the fold enrichment of *AES*, *B4GAT1*, and *MRPL11* transcripts, respectively, in DHX30-WT compared to p.Arg493His precipitates. Vertical lines indicate SD.

which we predicted to be responsible for ATP binding and/or hydrolysis. Namely, c.1685A>G, (p.His562Arg) identified in a single individual affects motif II, also referred to as Walker B motif, which binds β and γ phosphate and coordinates ATP hydrolysis.[19] Further, c.2342G>A, (p.Gly781Asp), identified in two individuals, c.2344C>T, (p.Arg782Trp), identified in three individuals, c.2353C>T, (p.Arg785Cys), also identified in three individuals, and c.2354G>A, (p.Arg785His), unique, all result in amino acid alterations residing in motif VI that binds γ phosphate and coordinates, together with motifs I and II, ATP binding and hydrolysis in other DExH family members[19,21] (Figure 1). Indeed, both Arg782 and Arg785 correspond to arginine residues that directly contact the γ phosphate.[1] Further evidence for the functional relevance of these highly conserved residues comes from *in vivo* analyses of the RH Prp43 in *Saccharomyces cerevisiae*. Substitutions of Arg150 and His218, the corresponding residues in the yeast protein to Arg493 and His562 in human DHX30 (Figure S2B), results in a cold sensitive growth retardation.[22,23] Similarly, the separate exchange of either Gly426, Arg427, and Arg430, corresponding to Gly781, Arg782, and Arg785 in DHX30, respectively (Figure S2B), is lethal.[22]

In line with the functional importance of the six residues affected in our allelic series, it is worth noting that all *DHX30* mutations identified herein are exceedingly rare; none of them is present in dbSNP, 1000 Genomes, or the ExAC or the gnomAD browser, indicating that they represent rare variants. In addition, based on the ExAC sequencing data, *DHX30* is predicted to be very intolerant to missense mutations, ranked 31 out of 18.000 analyzed genes by its missense *Z* score of 6.82,[24] which is even higher than the average *Z* score for genes involved in develop-

mental disorders.[25] Taken together, the genetic data, especially the recurrence of mutations, supported by published structural and functional data on other RHs provide strong evidence for the pathogenicity of the identified mutations.

During murine embryogenesis, *Dhx30/HelG* is strongly expressed in neural cells, and its biallelic loss leads to perinatal lethality in mice exhibiting early development defects in the central nervous system.[26] Therefore, *DHX30* constitutes an excellent candidate gene for human neurodevelopmental disorders. In an international large-scale sequencing study, we recently reported four of the individuals presented herein and suggested *DHX30* to be a plausible candidate gene for developmental disorders.[17] However, given the large size of the previous study, the corresponding clinical picture remained unclear, and none of the reported alterations was scrutinized by an experimental approach.

Therefore, to corroborate our findings, we developed an ATPase assay using transiently transfected HEK293T cells. To assess whether wild-type DHX30 (DHX30-WT) acts as an RNA-dependent ATPase, we immunoprecipitated DHX30-GFP and incubated it with ATP in the presence or absence of RNA. Indeed, ATPase activity, determined by a progressive increase of free phosphate concentration *in vitro*, was significantly stimulated by adding RNA, thus showing that DHX30 hydrolyses ATP in an RNA-dependent fashion (Figure 2A). When compared to DHX30-WT, all protein variants harboring amino acid substitutions in ATP binding motifs II and VI (p.His562Arg, p.Gly781Asp, p.Arg782Trp, p.Arg785Cys, and p.Arg785His) exhibit markedly reduced ATPase activities (Figure 2B). These data confirm our structural predictions and provide strong evidence for the pathogenicity of the respective mutations. Noteworthy, the p.Arg493His amino acid exchange
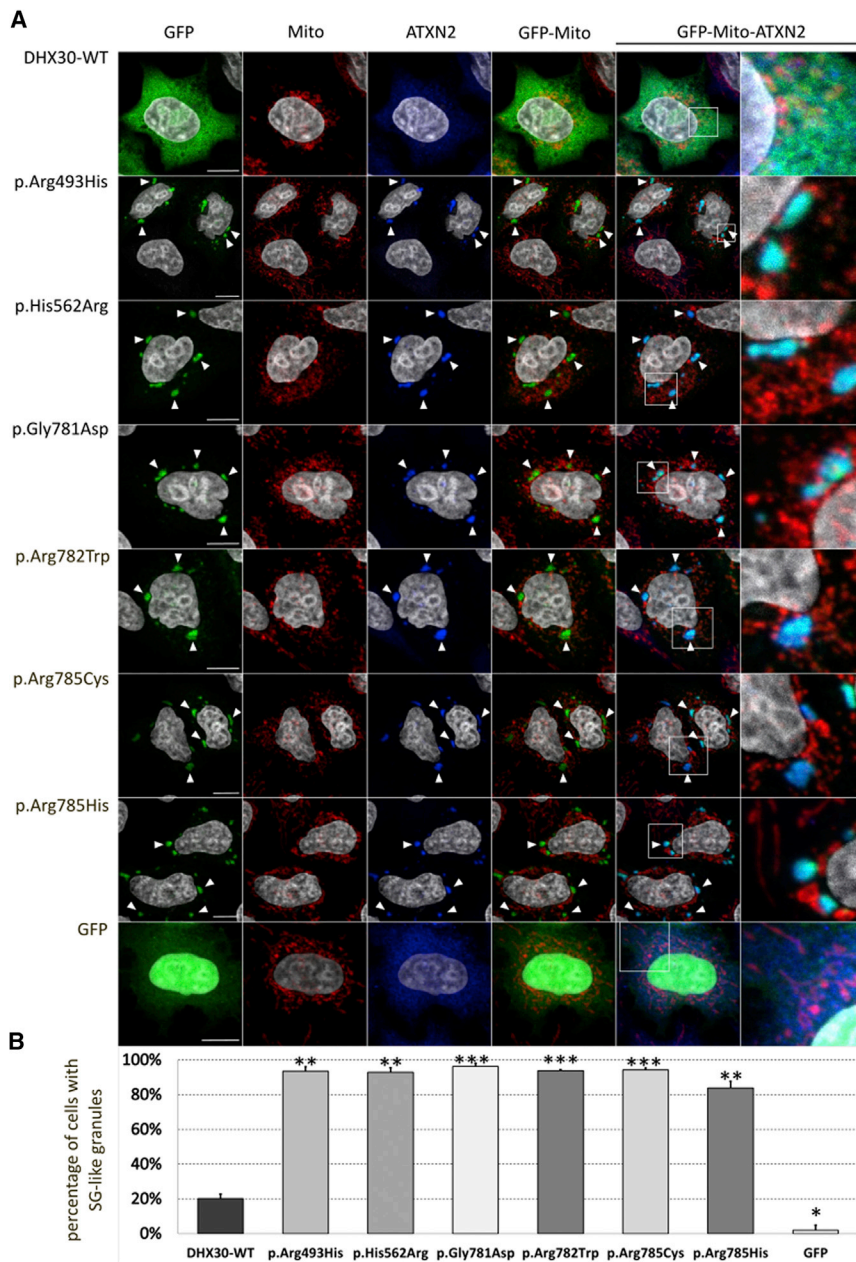
Figure 3. Recombinant Protein Variants of DHX30 Initiate the Formation of SG-like Cytoplasmic Aggregates

(A) Immunocytochemical detection of DHX30-GFP fusion proteins (GFP, green), mitochondria (Mito, red), and endogenous ATXN2 (blue) in transfected U2OS cells. Regions shown at high magnification in the rightmost panels are indicated by boxes. Whereas wild-type DHX30-GFP preferentially resides throughout the cytoplasm and GFP accumulates in nuclei, recombinant protein variants of DHX30 induce the genesis of cytoplasmic foci containing endogenous SG-marker ATXN2 (arrowheads). Nuclei are identified via DAPI staining (gray).

(B) Bar graph indicating the percentage of transfected cells, in which recombinant GFP proteins induce the emergence of SG-like structures. Vertical bars indicate SD. Statistical analysis was performed using unpaired Student's t test to individually compare each protein variant to wild-type DHX30-GFP (*p < 0.05; **p < 0.01; ***p < 0.001; n > 300 from two independent transfections).
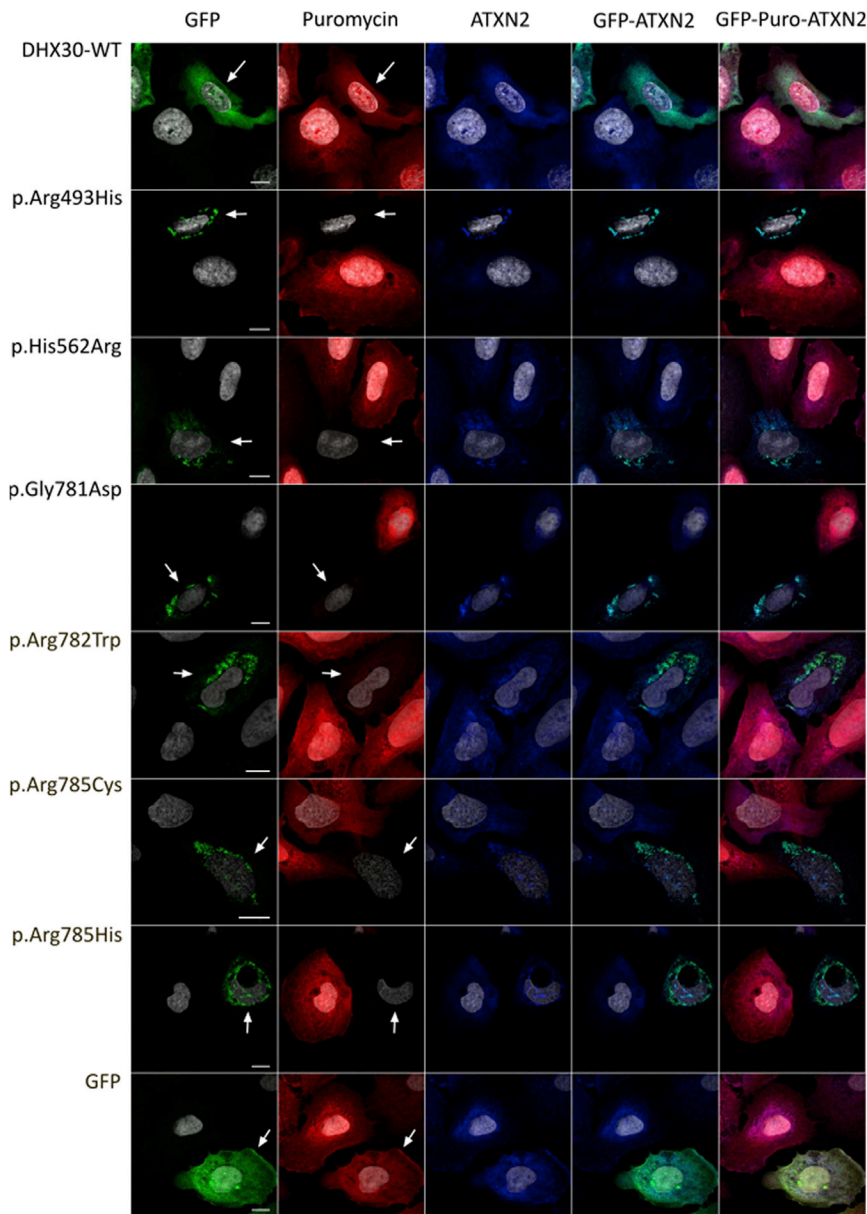
DHX30. Importantly, only negligible amounts of the three investigated transcripts co-purified with the GFP-mCherry control protein (Figure 2C and Figure S4). These data indicate that the p.Arg493His exchange in DHX30 strongly interferes with its *in vivo* binding capacity to certain target RNAs, yet does not completely abolish RNA recognition.

Next, we investigated the subcellular localization of WT and protein variants of DHX30 in U2OS cells. GFP-tagged DHX30-WT was mostly diffusely localized throughout the cytoplasm (Figure 3) with a slight accumulation in mitochondria, consistent with the distribution of endogenous DHX30 (Figure S5A) and previous findings.[30] In contrast, in the majority of transfected cells all protein variants strongly accumulated in discrete cytoplasmic foci (> 80%; Figure 3), which were identified as SGs via co-labeling with Ataxin-2 (*ATXN2*, MIM: 601517), a well-established SG marker.[31] SGs are cytoplasmic RNPs that form in cells during stress responses when translation initiation rates of most mRNAs are decreased.[32] Remarkably, in response to heat stress endogenous DHX30 also alters its diffuse cytoplasmic localization to accumulate in SGs (Figure S5B). These findings show that independent from exogenous stressors, protein variants of DHX30 exhibit a strongly increased propensity to induce SG assembly compared to DHX30-WT. To further determine if SG formation induced by DHX30 protein variants alters protein synthesis, we monitored global translation rates in transfected versus untransfected U2OS cells. In this assay, puromycin incorporation into newly synthesized peptides directly reflects the translation rate and can be visualized via immunocytochemistry.[33] While expression of all tested

affecting the putative RNA-binding motif Ia did not alter RNA-dependent ATPase activity of DHX30.

To analyze the impact of p.Arg493His on RNA binding, we performed an RNA immunoprecipitation analysis with transfected HEK293T cells.[18] For this, RNP complexes containing recombinant DHX30-WT or p.Arg493His, respectively, were affinity purified and subjected to quantitative real-time RT-PCR to examine the presence of three distinct putative target mRNAs. Targets were randomly selected from a publicly available eCLIP (enhanced version of the crosslinking and immunoprecipitation) dataset obtained in HepG2 cells (accession ENCSR565DGW), generated by the ENCODE project.[27–29] A detailed view of the respective DHX30 eCLIP hits is shown in Figure S3. We determined that the p.Arg493His amino acid substitution leads to a 9- to 11-fold decrease in the amount of *AES* (MIM: 600188), *B4GAT1* (MIM: 605517), and *MRPL11* (MIM: 611826) mRNAs associated with

Figure 4. SG Formation Initiated by Protein Variants of DHX30 Selectively Inhibits Global Translation in Transfected U2OS Cells

Puromycin incorporation assay in U2OS cells expressing DHX30-GFP fusion proteins (GFP, green). Translation is monitored by staining against puromycin (Puro, red), SGs are detected by ATXN2 (blue) and nuclei via DAPI staining (gray). While cells expressing wild-type DHX30-GFP or GFP display puromycin labeling comparable to neighboring untransfected cells, puromycin incorporation is strongly diminished in cells expressing recombinant protein variants of DHX30. Arrows indicate transfected cells. Note the correlation between SG assembly and lack of puromycin staining.

tional role for DHX30 related to SG assembly and global translation control. Notably, aberrant SG assembly and clearance with concomitant global translation impairment have been observed in a broad range of neurodegenerative and neurodevelopmental diseases. Examples include amyotrophic lateral sclerosis and frontotemporal dementia (MIM: 612069),[36] spinocerebellar ataxia type 2 (MIM: 183090),[31] Fragile X syndrome (MIM: 300624)[37,38] and Renpenning syndrome (MIM: 309500).[39] Indeed, accurate translation throughout development has recently emerged as a key factor for proper formation and maintenance of complex neural circuits,[40] thereby regulating learning, memory, and behavior. Notably, SGs temporarily arrest mRNA translation upon both exogenous and endogenous stressors.[32] Because the human organism is, even *in utero*, under constant exposure to both endogenous and exogenous stressors, we hypothesize that the mutations identified here generate a chronic condition whereby pervasive and pronounced SG hyper-assembly induces impairments in the local regulation of translation.

recombinant DHX30 protein variants dramatically decreased puromycin incorporation compared to neighboring untransfected cells, puromycin labeling of cells expressing DHX30-WT was similar to that of untransfected cells (Figure 4). Taken together, the above data suggest that protein variants of DHX30 significantly increased the propensity of stress granule formation and thus lead to a global decrease in protein synthesis.

Discussion

Most RHs are involved in several, non-mutually exclusive aspects of RNA metabolism. Similarly, DHX30 was suggested to control different phases of the RNA life cycle as well as ribosome assembly in mitochondria.[30,34,35] However, none of the affected individuals presented here displays clear clinical signs of mitochondriopathies. Thus, it is rather unlikely that the mutations identified here primarily affect mitochondrial function. Actually, our *in vitro* characterization of these mutations has uncovered an addi-

Whereas we show a distinct molecular defect for each DHX30 variant with respect to either RNA binding or ATPase activity, one might also speculate that disease-associated sequence alterations in DHX30 could affect protein folding or stability. Indeed, protein levels of GFP-tagged variants are somewhat reduced when compared to WT DHX30, as evident from both fluorescence microscopy (Figures 3 and 4) and western blots of lysates of transfected cells (Figure S6). However, this reduced accumulation level might actually be caused by the induction of SGs which is observed upon expression of *DHX30* variants. As SG formation leads to reduced general translation, DHX30 variants (but not the WT protein) might indeed limit their own production. Given that DHX30-WT is readily incorporated into SGs e.g., upon heat stress, we assume that also the endogenous DHX30 protein is present in SGs upon expression of variant forms of the protein. These

findings might point to a possible dominant negative effect of the mutations identified here.

Interestingly, homozygous deficiency of HelG/DHX30 in mice results in early embryonic lethality, whereas heterozygous mice are apparently normal and fertile.[26] However, no in-depth phenotypic analysis of heterozygous mice, including behavioral tests for learning and memory formation, has been performed up to date. Thus, the so-far published data on DHX30-deficient mice do not allow for a direct comparison of phenotypes with the individuals described here. Nevertheless, they might indicate that the missense mutations described in our study might have a more severe effect than the loss of one copy of the gene.

In conclusion, we report that heterozygous missense mutations in *DHX30* cause a syndrome characterized by GDD, ID, severe speech impairment and gait abnormalities, and highlight the role of proper translation in neurodevelopment.

Supplemental Data

Supplemental Data include five figures and Supplemental Experimental Procedures and can be found with this article online at https://doi.org/10.1016/j.ajhg.2017.09.014.

Data Availability

The identified *DHX30* variants have been deposited to the Leiden Open (source) Variation Database (LOVD) (https://databases.lovd.nl/shared/variants/DHX30/unique) under following accession numbers: 0000195646, 0000195647, 0000195648, 0000195649, 0000195650, 0000195651, 0000195652, and 0000195653. The raw whole-exome sequencing data that support the findings in affected individual cannot be made publicly available for reasons of affected individuals' confidentiality. Qualified researchers may apply for access to these data, pending institutional review board approval. All other data generated or analyzed during this study are included in this published article (and its Supplemental Data files).

Web Resources

1000 Genomes, http://browser.1000genomes.org/index.html
dbSNP, https://www.ncbi.nlm.nih.gov/projects/SNP/
ENCODE, https://www.encodeproject.org/
Ensembl Genome Browser, http://www.ensembl.org/index.html
ExAC Browser, http://exac.broadinstitute.org/
gnomAD Browser, http://gnomad.broadinstitute.org/
OMIM, http://www.omim.org/

References

1. Linder, P., and Jankowsky, E. (2011). From unwinding to clamping - the DEAD box RNA helicase family. Nat. Rev. Mol. Cell Biol. *12*, 505–516.
2. Jankowsky, E. (2011). RNA helicases at work: binding and rearranging. Trends Biochem. Sci. *36*, 19–29.
3. Laggerbauer, B., Achsel, T., and Lührmann, R. (1998). The human U5-200kD DEXH-box protein unwinds U4/U6 RNA duplices in vitro. Proc. Natl. Acad. Sci. USA *95*, 4188–4192.
4. Umate, P., Tuteja, N., and Tuteja, R. (2011). Genome-wide comprehensive analysis of human helicases. Commun. Integr. Biol. *4*, 118–137.
5. Valentin-Vega, Y.A., Wang, Y.D., Parker, M., Patmore, D.M., Kanagaraj, A., Moore, J., Rusch, M., Finkelstein, D., Ellison, D.W., Gilbertson, R.J., et al. (2016). Cancer-associated *DDX3X* mutations drive stress granule assembly and impair global translation. Sci. Rep. *6*, 25996.
6. Snijders Blok, L., Madsen, E., Juusola, J., Gilissen, C., Baralle, D., Reijnders, M.R., Venselaar, H., Helsmoortel, C., Cho, M.T., Hoischen, A., et al.; DDD Study (2015). Mutations in *DDX3X* Are a Common Cause of Unexplained Intellectual Disability with Gender-Specific Effects on Wnt Signaling. Am. J. Hum. Genet. *97*, 343–352.
7. Sobreira, N., Schiettecatte, F., Boehm, C., Valle, D., and Hamosh, A. (2015). New tools for Mendelian disease gene identification: PhenoDB variant analysis module; and GeneMatcher, a web-based tool for linking investigators with an interest in the same gene. Hum. Mutat. *36*, 425–431.
8. Hempel, M., Cremer, K., Ockeloen, C.W., Lichtenbelt, K.D., Herkert, J.C., Denecke, J., Haack, T.B., Zink, A.M., Becker, J., Wohlleber, E., et al. (2015). De Novo Mutations in *CHAMP1* Cause Intellectual Disability with Severe Speech Impairment. Am. J. Hum. Genet. *97*, 493–500.
9. Küry, S., Besnard, T., Ebstein, F., Khan, T.N., Gambin, T., Douglas, J., Bacino, C.A., Craigen, W.J., Sanders, S.J., Lehmann, A., et al. (2017). De Novo Disruption of the Proteasome

Regulatory Subunit *PSMD12* Causes a Syndromic Neurodevelopmental Disorder. Am. J. Hum. Genet. *100*, 352–363.

10. Ta-Shma, A., Zhang, K., Salimova, E., Zernecke, A., Sieiro-Mosti, D., Stegner, D., Furtado, M., Shaag, A., Perles, Z., Nieswandt, B., et al. (2017). Congenital valvular defects associated with deleterious mutations in the *PLD1* gene. J. Med. Genet. *54*, 278–286.

11. Isidor, B., Küry, S., Rosenfeld, J.A., Besnard, T., Schmitt, S., Joss, S., Davies, S.J., Lebel, R.R., Henderson, A., Schaaf, C.P., et al. (2016). De Novo Truncating Mutations in the Kinetochore-Microtubules Attachment Gene *CHAMP1* Cause Syndromic Intellectual Disability. Hum. Mutat. *37*, 354–358.

12. Deciphering Developmental Disorders, S.; and Deciphering Developmental Disorders Study (2015). Large-scale discovery of novel genetic causes of developmental disorders. Nature *519*, 223–228.

13. Banuelos, E., Ramsey, K., Belnap, N., Krishnan, M., Balak, C., Szelinger, S., Siniard, A.L., Russell, M., Richholt, R., De Both, M., et al. (2017). Case Report: Novel mutations in *TBC1D24* are associated with autosomal dominant tonic-clonic and myoclonic epilepsy and recessive Parkinsonism, psychosis, and intellectual disability. F1000Res. *6*, 553.

14. Kleefstra, T., Kramer, J.M., Neveling, K., Willemsen, M.H., Koemans, T.S., Vissers, L.E., Wissink-Lindhout, W., Fenckova, M., van den Akker, W.M., Kasri, N.N., et al. (2012). Disruption of an EHMT1-associated chromatin-modification module causes intellectual disability. Am. J. Hum. Genet. *91*, 73–82.

15. de Ligt, J., Willemsen, M.H., van Bon, B.W., Kleefstra, T., Yntema, H.G., Kroes, T., Vulto-van Silfhout, A.T., Koolen, D.A., de Vries, P., Gilissen, C., et al. (2012). Diagnostic exome sequencing in persons with severe intellectual disability. N. Engl. J. Med. *367*, 1921–1929.

16. Farwell, K.D., Shahmirzadi, L., El-Khechen, D., Powis, Z., Chao, E.C., Tippin Davis, B., Baxter, R.M., Zeng, W., Mroske, C., Parra, M.C., et al. (2015). Enhanced utility of family-centered diagnostic exome sequencing with inheritance model-based analysis: results from 500 unselected families with undiagnosed genetic conditions. Genet. Med. *17*, 578–586.

17. Eldomery, M.K., Coban-Akdemir, Z., Harel, T., Rosenfeld, J.A., Gambin, T., Stray-Pedersen, A., Küry, S., Mercier, S., Lessel, D., Denecke, J., et al. (2017). Lessons learned from additional research analyses of unsolved clinical exome cases. Genome Med. *9*, 26.

18. Miroci, H., Schob, C., Kindler, S., Ölschläger-Schütt, J., Fehr, S., Jungenitz, T., Schwarzacher, S.W., Bagni, C., and Mohr, E. (2012). Makorin ring zinc finger protein 1 (MKRN1), a novel poly(A)-binding protein-interacting protein, stimulates translation in nerve cells. J. Biol. Chem. *287*, 1322–1334.

19. Tanner, N.K., and Linder, P. (2001). DExD/H box RNA helicases: from generic motors to specific dissociation functions. Mol. Cell *8*, 251–262.

20. Tauchert, M.J., Fourmann, J.B., Lührmann, R., and Ficner, R. (2017). Structural insights into the mechanism of the DEAH-box RNA helicase Prp43. eLife *6*, 6.

21. Caruthers, J.M., and McKay, D.B. (2002). Helicase structure and mechanism. Curr. Opin. Struct. Biol. *12*, 123–133.

22. Martin, A., Schneider, S., and Schwer, B. (2002). Prp43 is an essential RNA-dependent ATPase required for release of lariat-intron from the spliceosome. J. Biol. Chem. *277*, 17743–17750.

23. Tanaka, N., and Schwer, B. (2006). Mutations in PRP43 that uncouple RNA-dependent NTPase activity and pre-mRNA splicing function. Biochemistry *45*, 6510–6521.

24. Lek, M., Karczewski, K.J., Minikel, E.V., Samocha, K.E., Banks, E., Fennell, T., O'Donnell-Luria, A.H., Ware, J.S., Hill, A.J., Cummings, B.B., et al.; Exome Aggregation Consortium (2016). Analysis of protein-coding genetic variation in 60,706 humans. Nature *536*, 285–291.

25. Samocha, K.E., Robinson, E.B., Sanders, S.J., Stevens, C., Sabo, A., McGrath, L.M., Kosmicki, J.A., Rehnström, K., Mallick, S., Kirby, A., et al. (2014). A framework for the interpretation of de novo mutation in human disease. Nat. Genet. *46*, 944–950.

26. Zheng, H.J., Tsukahara, M., Liu, E., Ye, L., Xiong, H., Noguchi, S., Suzuki, K., and Ji, Z.S. (2015). The novel helicase helG (DHX30) is expressed during gastrulation in mice and has a structure similar to a human DExH box helicase. Stem Cells Dev. *24*, 372–383.

27. Van Nostrand, E.L., Pratt, G.A., Shishkin, A.A., Gelboin-Burkhart, C., Fang, M.Y., Sundararaman, B., Blue, S.M., Nguyen, T.B., Surka, C., Elkins, K., et al. (2016). Robust transcriptome-wide discovery of RNA-binding protein binding sites with enhanced CLIP (eCLIP). Nat. Methods *13*, 508–514.

28. Consortium, E.P.; and ENCODE Project Consortium (2012). An integrated encyclopedia of DNA elements in the human genome. Nature *489*, 57–74.

29. Sloan, C.A., Chan, E.T., Davidson, J.M., Malladi, V.S., Strattan, J.S., Hitz, B.C., Gabdank, I., Narayanan, A.K., Ho, M., Lee, B.T., et al. (2016). ENCODE data at the ENCODE portal. Nucleic Acids Res. *44* (D1), D726–D732.

30. Wang, Y., and Bogenhagen, D.F. (2006). Human mitochondrial DNA nucleoids are linked to protein folding machinery and metabolic enzymes at the mitochondrial inner membrane. J. Biol. Chem. *281*, 25791–25802.

31. Nonhoff, U., Ralser, M., Welzel, F., Piccini, I., Balzereit, D., Yaspo, M.L., Lehrach, H., and Krobitsch, S. (2007). Ataxin-2 interacts with the DEAD/H-box RNA helicase DDX6 and interferes with P-bodies and stress granules. Mol. Biol. Cell *18*, 1385–1396.

32. Mahboubi, H., and Stochaj, U. (2017). Cytoplasmic stress granules: Dynamic modulators of cell signaling and disease. Biochim. Biophys. Acta *1863*, 884–895.

33. Schmidt, E.K., Clavarino, G., Ceppi, M., and Pierre, P. (2009). SUnSET, a nonradioactive method to monitor protein synthesis. Nat. Methods *6*, 275–277.

34. Minczuk, M., He, J., Duch, A.M., Ettema, T.J., Chlebowski, A., Dzionek, K., Nijtmans, L.G., Huynen, M.A., and Holt, I.J. (2011). TEFM (c17orf42) is necessary for transcription of human mtDNA. Nucleic Acids Res. *39*, 4284–4299.

35. Antonicka, H., and Shoubridge, E.A. (2015). Mitochondrial RNA Granules Are Centers for Posttranscriptional RNA Processing and Ribosome Biogenesis. Cell Rep. February 12, 2015. https://doi.org/10.1016/j.celrep.2015.01.030.

36. Li, Y.R., King, O.D., Shorter, J., and Gitler, A.D. (2013). Stress granules as crucibles of ALS pathogenesis. J. Cell Biol. *201*, 361–372.

37. Vanderklish, P.W., and Edelman, G.M. (2005). Differential translation and fragile X syndrome. Genes Brain Behav. *4*, 360–384.

38. Gareau, C., Houssin, E., Martel, D., Coudert, L., Mellaoui, S., Huot, M.E., Laprise, P., and Mazroui, R. (2013). Characterization of fragile X mental retardation protein recruitment and dynamics in Drosophila stress granules. PLoS ONE *8*, e55342.

39. Kunde, S.A., Musante, L., Grimme, A., Fischer, U., Müller, E., Wanker, E.E., and Kalscheuer, V.M. (2011). The X-chromosome-linked intellectual disability protein PQBP1 is a component of neuronal RNA granules and regulates the appearance of stress granules. Hum. Mol. Genet. *20*, 4916–4931.

40. Darnell, J.C., and Richter, J.D. (2012). Cytoplasmic RNA-binding proteins and the control of complex brain function. Cold Spring Harb. Perspect. Biol. *4*, a012344.